ACS APPLIED NANO MATERIALS

www.acsanm.org Article

Branchless Colloidal PbSe Nanorods: Implications for Solution-Processed Optoelectronic and Thermoelectric Devices

Yiteng Tang, Shreedhar R. Kandel, Zhoufeng Jiang, Paul J. Roland, Randy Ellingson, and Liangfeng Sun*

Cite This: *ACS Appl. Nano Mater.* 2021, 4, 10708–10712 Read Online

ACCESS | Metrics & More | Article Recommendations | Supporting Information

ABSTRACT: Acetic acid causes branching of PbSe nanorods during the synthesis of colloidal PbSe nanorods. Removing acetic acid in the reaction solution prevents branching, resulting in uniform nanorods. It increases the photoluminescence quantum yield of the nanorods from 11% (branched) to 38% (branchless). The branchless nanorods exhibit single-exponential photoluminescence decay with a decay constant of 1.3 μs, in contrast to multiple-exponential photoluminescence decay in branched nanorods with an e-folding lifetime of 0.12 μs. The diameter of the nanorods can be tuned from 3.9 to 5.8 nm by changing the reaction temperature, resulting in an energy gap tunable from 0.88 to 0.65 eV. The dependence of the energy gap on the diameter follows the power law: diameter$^{-1.5}$. The superior optical properties, including long exciton lifetime, high photoluminescence quantum yield, and tunable energy gaps, make the branchless PbSe nanorods an excellent candidate material for thermoelectric and optoelectronic devices.

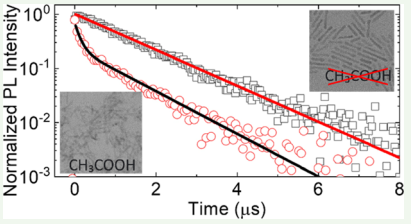

KEYWORDS: *PbSe nanorods, acetic acid, oriented attachment, tunable band gap, thermoelectric, optoelectronic*

INTRODUCTION

Owing to its high thermoelectric figure of merit, lead selenide (PbSe) is a promising thermoelectric material.[1−5] The anisotropic one-dimensional structure further enhances this property.[6,7] In contrast to zero-dimensional quantum dots, high carrier mobility and large diffusion length along the rod axis can be achieved by the one-dimensional geometry in optoelectronic applications.[8] Moreover, the high multiple exciton generation rate[9−12] and the slow Auger recombination rate[13,14] reported for nanorods make them promising for efficient photovoltaic devices.

Synthesis of uniform nanorods is essential for their applications. However, branched nanorods often appear in the final product of the synthesis, mixing with the branchless nanorods.[15,16] It is likely due to the existence of multiple mechanisms[16−19] that affect the growth of the nanorods. Some cosolvents (e.g., water) have a significant effect on the shape of the nanorods.[20] Placencia et al. demonstrated the synthesis of branchless nanorods by removing water from the reaction solution.[21]

In this study, we demonstrate that acetic acid has a significant effect on the branching of nanorods. By removing it from the reaction solution, we can synthesize branchless PbSe nanorods. The branchless nanorods have better optical properties than the branched nanorods, for instance, a higher photoluminescence quantum efficiency and a longer exciton lifetime. Our results also indicate that acetic acid promotes the anisotropic growth of PbSe nanorods and removing it from the reaction solution makes the one-dimensional oriented attachment to dominate the growth of the nanorods.

EXPERIMENTS AND RESULTS

In our earlier synthesis of PbSe nanorods, lead acetate was used as the lead precursor.[16] We noticed that the PbSe nanorods are all branched at reaction temperatures ranging from 110 to 180 °C. At certain temperatures (e.g., 180 °C), aggregated nanorods form (Supporting Information A). We speculated that acetic acid—a byproduct in the preparation of the lead precursor, as shown in eq 1—affected the growth of nanorods:

$$Pb(CH_3COO)_2 \cdot 3H_2O + 2C_{18}H_{34}O_2 \rightarrow Pb(C_{18}H_{32}O_2)_2 + 2CH_3COOH + 3H_2O \quad (1)$$

Acetate salts play an important role in the syntheses of CdX (X = S, Se, or Te) nanoplatelets[22,23]—a two-dimensional structure. However, in the synthesis of colloidal PbS nanosheets, acetic acid causes aggregation of the nanosheets and ruins the synthesis.[24] A trace amount of acetate in the reaction solution leads to star-shaped nanocrystals during the synthesis of PbSe quantum dots.[25] In the synthesis of PbSe nanorods described by the reaction equation (eq 1), we reduced acetic acid and water from the reaction solution by degassing. However, the PbSe nanorods are still branched, which is probably caused by the residual acetic acid.

To avoid acetic acid as the byproduct in the reaction, the reactant—lead acetate—is replaced by lead oxide (Supporting Information B). In this acetate-free method, as shown in Scheme 1, the synthesized PbSe nanorods are branchless. Nanorods with a

Received: July 27, 2021
Accepted: September 9, 2021
Published: September 21, 2021

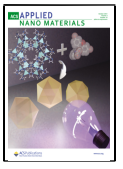

https://doi.org/10.1021/acsanm.1c02123
ACS Appl. Nano Mater. 2021, 4, 10708–10712

Scheme 1. Reaction of Lead Oxide with Oleic Acid Produces Lead Oleate and Water (No Acetic Acid)

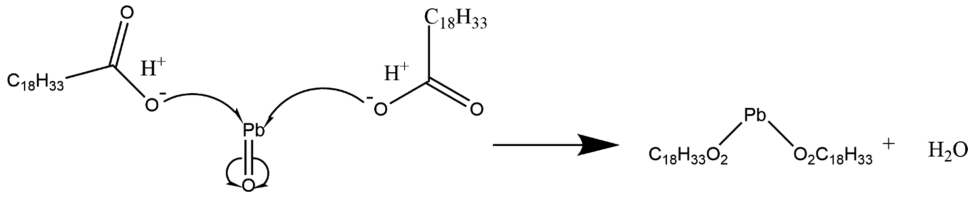

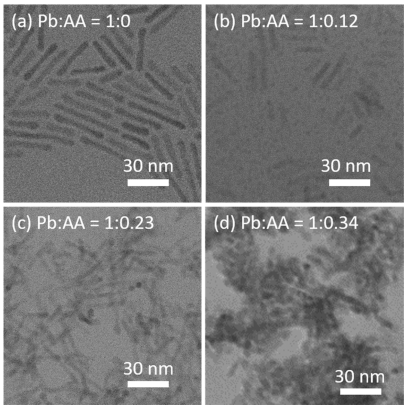

Figure 1. TEM images of PbSe nanorods synthesized at 130 °C with different lead (Pb) to acetic acid (AA) ratios: (a) 1:0, (b) 1:0.12, (c) 1:0.23, and (d) 1:0.34.

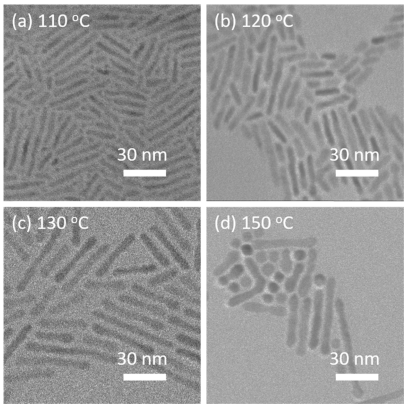

Figure 2. TEM images of PbSe nanorods synthesized using the AA-free method at reaction temperatures of (a) 110 °C, (b) 120 °C, (c) 130 °C, and (d) 150 °C, respectively.

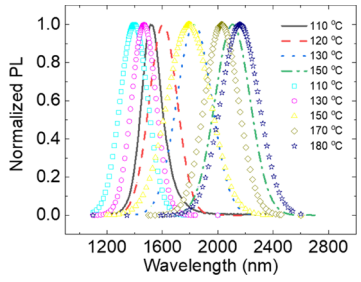

Figure 3. Photoluminescence (PL) spectra of PbSe nanorods synthesized at different temperatures using the method with (symbols) or without (lines) AA.

uniform diameter are observed using a transmission electron microscope (TEM) (Figure 1a).

To understand the effect of acetic acid, we conducted a systematic study of the synthesis by injecting different amounts of acetic acid into the reaction solution each time. When 15 μL of acetic acid (molar ratio lead:acetic acid = 1:0.12) is injected into the reaction solution, small quantum dots and thin nanorods appear in the product (Figure 1b). If the injected acetic acid is doubled (lead:acetic acid = 1:0.23), the product shows branched nanorods (Figure 1c). As the injected acetic acid reached 45 μL, the nanocrystals aggregated, showing clusters in the TEM image (Figure 1d). Addition of more acetic acid results in the same clusters (Supporting Information C). In addition to the formation of branched nanorods, the diameter of the nanorods decreases with the increase of the amount of acetic acid. This can be seen in the TEM images (Figure 1). The blueshift of the photoluminescence by the increase of acetic acid confirms the trend (Supporting Information D).

There are two different growth mechanisms for PbSe nanorods: one-dimensional oriented attachment[19] and anisotropic growth.[16] The oriented attachment is one of the important mechanisms for the growth of two-dimensional[26,27] as well as one-dimensional[17] colloidal nanostructures. In our previous research, one-dimensional oriented attachment caused by the electric dipolar interaction[19] was introduced to explain the growth of PbSe nanorods. An electric dipole can form within a PbSe nanocrystal if the two opposite (111) facets are terminated by either Pb or selenium (Se) atoms.[17] When chloroalkane—an important cosolvent for the growth of two-dimensional PbS nanosheets[26]—is added as a cosolvent, it reduces the growth rate of the nanocrystal[16,19] so that the electric dipolar interaction between the nanocrystals has enough time to align and attach the nanocrystal. When AA is present in the reaction solution, the growth of the nanocrystal is faster (Supporting Information E). The AA molecule has the same carboxyl group (COOH) as the oleic acid molecule but a shorter carbon chain. The AA ligands can replace the oleic acid ligands on the nanocrystal surface, thus reducing the steric hindrance, making the nanocrystal surface more reactive. A similar trend has been reported when the long surface ligands—trioctylphosphine—are replaced by the short surface ligands—tris(diethylamino)phosphine—in the synthesis of PbSe nanorods.[28] The anisotropic growth of the nanocrystal will occur due to the increased reactivity, resulting in branched nanorods.[16] More AA increases the growth rate further, causing more branching and aggregation. In the literature, more fundamental studies of the interaction between the surface ligands and the nanocrystals (e.g., PbS nanocrystals) show that the interaction affects the nanocrystal shape as well as the superlattice structure made up of the nanocrystals.[29,30]

The reaction temperature affects the morphology of the nanorods in both syntheses with and without AA. The diameter of the nanorod increases as the reaction temperature increases in both cases. The length of the nanorod reaches the maximum at 150 °C in the synthesis with AA (Supporting Information A). Beyond 150 °C, higher reaction temperatures result in short branched nanorods (170 °C) or nanorod clusters (180 °C). In the AA-free synthesis, the length of the nanorods is nearly the same at reaction temperatures ranging from 110 to 130 °C (Figure 2a–c). However, at a higher temperature (150 °C), shorter nanorods and nanodots start to appear (Figure 2d). The thermodynamically controlled growth likely starts to take over at 150 °C, while the kinetically controlled growth dominates at lower temperatures.[19] At a higher temperature of 170 °C, however, long zigzag nanowires are formed (Supporting Information F). The octahedral PbSe QDs likely formed and attached along the <100> direction.[17] At temperatures of 110, 130, and 150 °C, respectively, both syntheses (with and without AA) are carried out under the same reaction conditions, but the octahedral PbSe QDs show branching

https://doi.org/10.1021/acsanm.1c02123
ACS Appl. Nano Mater. 2021, 4, 10708−10712

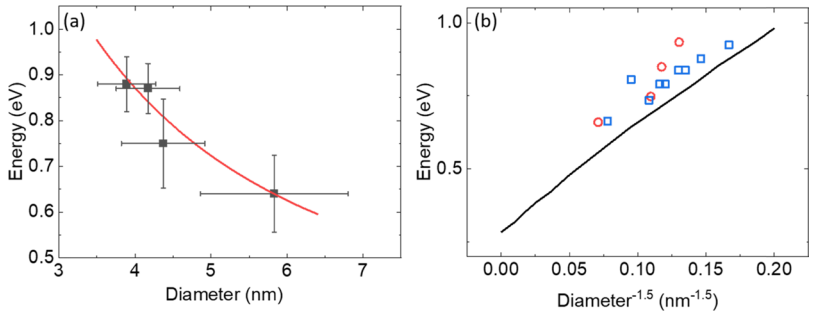

Figure 4. (a) Diameter-dependent energy gap. The data (solid squares) are fit based on the quantum confinement model (solid line). (b) Dependence of the energy gap on the diameter of the nanorods. Both this study (circles) and Bartnik's data (squares) follow the trend predicted by the four-band ***k·p*** model.[32]

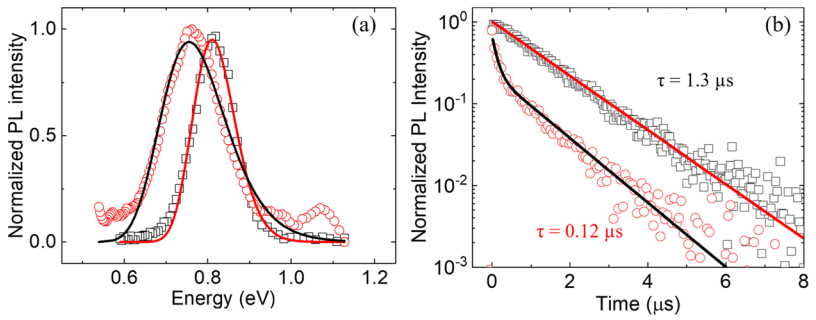

Figure 5. (a) PL spectra of the branched (circles) and the branchless (squares) PbSe nanorods fit by a Gaussian function, respectively. (b) Time-resolved PL decay traces of branched (circles) and branchless (squares) PbSe nanorods.

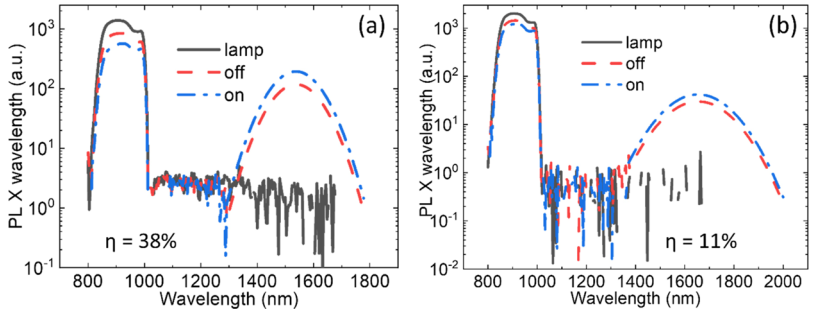

Figure 6. Measurements of the absolute PL quantum yields of (a) branchless and (b) branched PbSe nanorods. For each measurement, three scans were taken: excitation beam only (solid line), sample off the excitation beam (dashed line), and sample on the excitation beam (dash-dotted line). The excitation wavelength ranges from 800 to 1000 nm. The PL appears at wavelengths beyond 1300 nm.

with AA (Supporting Information A) and are branchless without AA (Figure 2).

The central wavelengths of the photoluminescence of the PbSe nanorods are different when they are synthesized at different reaction temperatures. In either AA-free or with AA synthesis, a higher reaction temperature typically results in a smaller energy gap. This is confirmed by the redshift of the photoluminescence peak at an elevated reaction temperature. As shown in Figure 3, the peak wavelength consistently increases from 1393 to 2163 nm as the reaction temperature increases from 110 to 180 °C.

The redshift of the PL peak indicates the decrease of the energy gap of the nanorods. It is likely caused by the increase in the diameter of the nanorod as shown by the TEM images (Figure 2). Since the typical length of the nanorod is 30 nm and above, the quantum confinement in the length direction is not significant.[31] Therefore, the change of the energy gap is mainly due to the change of the diameter.

To find out the quantitative dependence of the energy gap on the nanorod diameter, we measured the diameter and the energy gap of the nanorods synthesized at different temperatures. Both branched and branchless nanorods show longer PL peak wavelengths with larger diameters (Supporting Information G). We use only the branchless nanorods to find out the relation between the energy gap and the diameter while avoiding the complication caused by branching. The diameters of the PbSe nanorods were measured from the TEM images (Supporting Information H) and their energy gaps were determined using the optical absorption peaks (Supporting Information I).

The average energy gap of the nanorods decreases from 0.88 to 0.65 eV as their average diameter increases from 3.9 to 5.8 nm (Figure 4a). The diameter-dependent energy gap of the nanorods is described by the quantum confinement model

$$E_{gap}(d) = E_{gap}(\infty) + \frac{1}{0.17d^{1.5} + 0.29} \quad (2)$$

where $E_{gap}(d)$ is the energy gap of the nanorods of diameter d, and $E_{gap}(\infty)$ is the energy gap of bulk PbSe at room temperature, which is 0.27 eV.[33] The colloidal PbSe nanorods synthesized using other methods[21,31] also have the same diameter-dependent energy gap as described by the above equation (Supporting Information J).

Using the four-band ***k·p*** model, Bartnik and co-workers have calculated that the dependence of the energy gap on the diameter follows the power law: $E_g \propto d^{-1.5}$, where E_g is the energy gap and d is

https://doi.org/10.1021/acsanm.1c02123
ACS Appl. Nano Mater. 2021, 4, 10708−10712

the diameter.[32] Our experimental data and Bartnik's data follow the power law predicted by the model (Figure 4b).

In contrast to the branched nanorods (Figure 1c), the branchless PbSe nanorods (Figure 2a) have better optical properties. The PL peak from the branchless nanorods is well fit by a Gaussian function with a standard deviation σ_a of 0.06 eV (Figure 5a). The peak from the branched nanorods can be fit by a Gaussian function too but with a less fitting quality (Figure 5a). Its standard deviation σ_b is 0.09 eV, which is 50% larger than σ_a. Since the energy gap of the nanorod is mainly determined by the diameter of the nanorod, the broadening of the PL peak reflects the dispersion of the diameter of the nanorods. We use the ratio of standard deviation to the central photon energy (E) to represent the dispersion of the diameter. The dispersion of the branchless nanorod σ_a/E is about 7%, while the branched nanorods have a dispersion of 12%.

The time-resolved PL (Figure 5b) from the branchless PbSe nanorods shows a nearly single-exponential decay trace with an e-folding lifetime of 1.3 μs. It is more than 10 times longer than the e-folding lifetime (0.12 μs) of the branched nanorods. The decay trace of the latter exhibits two distinguished decay channels: a fast decay channel (τ_1 = 0.07 ± 0.01 μs, amplitude = 1.15) and a slow decay channel (τ_2 = 0.82 ± 0.02 μs, amplitude = 0.33). The fast decay channel may be due to charge trapping by the defects or the surface states. The single-exponential decay of PL by the branchless nanorods is close to that by PbSe quantum dots of the same energy gap[34] and similar to the results obtained by others.[18] The long exciton lifetime is important for optoelectronic applications such as photovoltaic devices since it provides more time for charge extraction and transport.

The PL quantum yield of the branchless PbSe nanorods is higher than that of the branched nanorods. Using our setup for measuring the absolute PL quantum yield[35,36] (Supporting Information K), we find that the quantum yield of the branchless PbSe nanorods is about 38%, three times more than that of the branched nanorods (11%) (Figure 6). This is consistent with the results from the PL lifetime measurements (Figure 5b).

CONCLUSIONS

In conclusion, we demonstrate the effect of AA on the synthesis of PbSe nanorods. Using the AA-free synthesis method, branchless PbSe nanorods can be obtained. The branchless PbSe nanorods show better optical properties including single-exponential decay, longer PL lifetime, and higher PL quantum yield. These superior properties make colloidal PbSe nanorods an excellent candidate material for optoelectronic and thermoelectric applications. By tuning the reaction temperature, the diameter and the energy gap of the PbSe nanorods can be systematically tuned. The dependence of the energy gap on the diameter follows the power law determined by the quantum confinement model.

ASSOCIATED CONTENT

Supporting Information

The Supporting Information is available free of charge at https://pubs.acs.org/doi/10.1021/acsanm.1c02123.

TEM images of PbSe nanorods, acetate-free synthesis of PbSe nanorods, AA effect, PL of PbSe nanorods, color-changing time, TEM images of synthesis at a high temperature, temperature-dependent diameters and PL, diameter of PbSe nanorods, optical absorption−temperature, diameter-dependent energy gap, and PL quantum yield (PDF)

AUTHOR INFORMATION

Corresponding Author

Liangfeng Sun − *Department of Physics and Astronomy and Center of Photochemical Sciences, Bowling Green State University, Bowling Green, Ohio 43403, United States;* orcid.org/0000-0003-0527-1777; Email: lsun@bgsu.edu

Authors

Yiteng Tang − *Department of Physics and Astronomy and Center of Photochemical Sciences, Bowling Green State University, Bowling Green, Ohio 43403, United States;* orcid.org/0000-0002-7533-756X

Shreedhar R. Kandel − *Department of Physics and Astronomy, Bowling Green State University, Bowling Green, Ohio 43403, United States*

Zhoufeng Jiang − *Department of Physics and Astronomy and Center of Photochemical Sciences, Bowling Green State University, Bowling Green, Ohio 43403, United States*

Paul J. Roland − *Department of Physics and Astronomy, Wright Center for Photovoltaic Innovation and Commercialization, School of Solar and Advanced Renewable Energy, University of Toledo, Toledo, Ohio 43606, United States*

Randy Ellingson − *Department of Physics and Astronomy, Wright Center for Photovoltaic Innovation and Commercialization, School of Solar and Advanced Renewable Energy, University of Toledo, Toledo, Ohio 43606, United States;* orcid.org/0000-0001-9520-6586

Complete contact information is available at: https://pubs.acs.org/10.1021/acsanm.1c02123

Notes

The authors declare no competing financial interest.

ACKNOWLEDGMENTS

This material is based on the work supported by the National Science Foundation under Grant No. 1905217. This work is partially supported with funding provided by the Office of the Vice President for Research & Economic Development, Bowling Green State University. L.S. thanks the funding provided by the U.S. Air Force Research Lab Summer Faculty Fellowship Program. We thank Charles Codding (machine shop) and Doug Martin (electronic shop) for their technical assistance at BGSU. The authors thank Joseph G. Lawrence for his help on the TEM measurements at the University of Toledo. P.R. and R.E. gratefully acknowledge the support of the Air Force Research Laboratory under contracts FA9453-08-C-0172 and FA9453-11-C-0253. R.E. acknowledges additional support from startup funds provided by the Wright Center for Photovoltaic Innovation and Commercialization.

REFERENCES

(1) Wang, H.; Pei, Y.; LaLonde, A. D.; Snyder, G. J. Weak electron−phonon coupling contributing to high thermoelectric performance in n-type PbSe. *Proc. Natl. Acad. Sci. U. S. A.* **2012**, *109*, 9705−9709.

(2) Androulakis, J.; Todorov, I.; He, J.; Chung, D.; Dravid, V.; Kanatzidis, M. Thermoelectrics from Abundant Chemical Elements: High-Performance Nanostructured PbSe−PbS. *J. Am. Chem. Soc.* **2011**, *133*, 10920−10927.

(3) Wang, H.; Pei, Y.; LaLonde, A. D.; Snyder, G. J. Heavily Doped p-Type PbSe with High Thermoelectric Performance: An Alternative for PbTe. *Adv. Mater.* **2011**, *23*, 1366−1370.

(4) Wang, H.; Gibbs, Z. M.; Takagiwa, Y.; Snyder, G. J. Tuning bands of PbSe for better thermoelectric efficiency. *Energy Environ. Sci.* **2014**, *7*, 804−811.
(5) Zhang, Q.; Wang, H.; Liu, W.; Wang, H.; Yu, B.; Zhang, Q.; Tian, Z.; Ni, G.; Lee, S.; Esfarjani, K.; Chen, G.; Ren, Z. Enhancement of thermoelectric figure-of-merit by resonant states of aluminium doping in lead selenide. *Energy Environ. Sci.* **2012**, *5*, 5246−5251.
(6) Zhao, Y.; Dyck, J. S.; Burda, C. Toward high-performance nanostructured thermoelectric materials: the progress of bottom-up solution chemistry approaches. *J. Mater. Chem.* **2011**, *21*, 17049−17058.
(7) Hicks, L. D.; Dresselhaus, M. S. Thermoelectric figure of merit of a one-dimensional conductor. *Phys. Rev. B* **1993**, *47*, 16631−16634.
(8) Graham, R.; Yu, D. High Carrier Mobility in Single Ultrathin Colloidal Lead Selenide Nanowire Field Effect Transistors. *Nano Lett.* **2012**, *12*, 4360−4365.
(9) Zhu, H.; Lian, T. Enhanced Multiple Exciton Dissociation from CdSe Quantum Rods: The Effect of Nanocrystal Shape. *J. Am. Chem. Soc.* **2012**, *134*, 11289−11297.
(10) Padilha, L. A.; Stewart, J. T.; Sandberg, R. L.; Bae, W. K.; Koh, W.; Pietryga, J. M.; Klimov, V. I. Aspect Ratio Dependence of Auger Recombination and Carrier Multiplication in PbSe Nanorods. *Nano Lett.* **2013**, *13*, 1092−1099.
(11) Cunningham, P. D.; Boercker, J. E.; Foos, E. E.; Lumb, M. P.; Smith, A. R.; Tischler, J. G.; Melinger, J. S. Enhanced Multiple Exciton Generation in Quasi-One-Dimensional Semiconductors. *Nano Lett.* **2011**, *11*, 3476−3481.
(12) Davis, N. J. L. K.; Böhm, M. L.; Tabachnyk, M.; Wisnivesky-Rocca-Rivarola, F.; Jellicoe, T. C.; Ducati, C.; Ehrler, B.; Greenham, N. C. Multiple-exciton generation in lead selenide nanorod solar cells with external quantum efficiencies exceeding 120%. *Nat. Commun.* **2015**, *6*, 8259.
(13) Aerts, M.; Spoor, F. C. M.; Grozema, F. C.; Houtepen, A. J.; Schins, J. M.; Siebbeles, L. D. A. Cooling and Auger Recombination of Charges in PbSe Nanorods: Crossover from Cubic to Bimolecular Decay. *Nano Lett.* **2013**, *13*, 4380−4386.
(14) Padilha, L. A.; Stewart, J. T.; Sandberg, R. L.; Bae, W. K.; Koh, W.; Pietryga, J. M.; Klimov, V. I. Carrier Multiplication in Semiconductor Nanocrystals: Influence of Size, Shape, and Composition. *Acc. Chem. Res.* **2013**, *46*, 1261−1269.
(15) Han, L.; Liu, J.; Yu, N.; Liu, Z.; Gu, J.; Lu, J.; Ma, W. Facile synthesis of ultra-small PbSe nanorods for photovoltaic application. *Nanoscale* **2015**, *7*, 2461−2470.
(16) Kandel, S. R.; Chiluwal, S.; Jiang, Z.; Tang, Y.; Roland, P. J.; Subedi, K.; Dimick, D. M.; Moroz, P.; Zamkov, M.; Ellingson, R.; Hu, J.; Voevodin, A. A.; Sun, L. One-dimensional growth of colloidal PbSe nanorods in chloroalkanes. *Phys. Status Solidi RRL* **2016**, *10*, 833−837.
(17) Cho, K. S.; Talapin, D. V.; Gaschler, W.; Murray, C. B. Designing PbSe nanowires and nanorings through oriented attachment of nanoparticles. *J. Am. Chem. Soc.* **2005**, *127*, 7140−7147.
(18) Koh, W. K.; Bartnik, A. C.; Wise, F. W.; Murray, C. B. Synthesis of monodisperse PbSe nanorods: a case for oriented attachment. *J. Am. Chem. Soc.* **2010**, *132*, 3909−3913.
(19) Tang, Y.; Premathilaka, S. M.; Weeraddana, T. M. D. S.; Kandel, S. R.; Jiang, Z.; Neupane, C. P.; Xi, H.; Wan, W.; Sun, L. Using Interaction of Nano Dipoles to Control the Growth of Nanorods. *J. Phys. Chem. Lett.* **2021**, *12*, 232−237.
(20) Boercker, J. E.; Foos, E. E.; Placencia, D.; Tischler, J. G. Control of PbSe Nanorod Aspect Ratio by Limiting Phosphine Hydrolysis. *J. Am. Chem. Soc.* **2013**, *135*, 15071−15076.
(21) Placencia, D.; Boercker, J. E.; Foos, E. E.; Tischler, J. G. Synthesis and Optical Properties of PbSe Nanorods with Controlled Diameter and Length. *J. Phys. Chem. Lett.* **2015**, *6*, 3360−3364.
(22) Ithurria, S.; Dubertret, B. Quasi 2D Colloidal CdSe Platelets with Thicknesses Controlled at the Atomic Level. *J. Am. Chem. Soc.* **2008**, *130*, 16504−16505.
(23) Ithurria, S.; Tessier, M. D.; Mahler, B.; Lobo, R. P. S. M.; Dubertret, B.; Efros, A. L. Colloidal nanoplatelets with two-dimensional electronic structure. *Nat. Mater.* **2011**, *10*, 936−941.
(24) Premathilaka, S. M.; Jiang, Z.; Antu, A.; Leffler, J.; Hu, J.; Roy, A.; Sun, L. A robust method for the synthesis of colloidal PbS nanosheets. *Phys. Status Solidi RRL* **2016**, *10*, 838−842.
(25) Houtepen, A. J.; Koole, R.; Vanmaekelbergh, D.; Meeldijk, J.; Hickey, S. G. The Hidden Role of Acetate in the PbSe Nanocrystal Synthesis. *J. Am. Chem. Soc.* **2006**, *128*, 6792−6793.
(26) Schliehe, C.; Juarez, B. H.; Pelletier, M.; Jander, S.; Greshnykh, D.; Nagel, M.; Meyer, A.; Foerster, S.; Kornowski, A.; Klinke, C.; Weller, H. Ultrathin PbS sheets by two-dimensional oriented attachment. *Science* **2010**, *329*, 550−553.
(27) Wang, Z.; Schliehe, C.; Wang, T.; Nagaoka, Y.; Cao, Y. C.; Bassett, W. A.; Wu, H.; Fan, H.; Weller, H. Deviatoric Stress Driven Formation of Large Single-Crystal PbS Nanosheet from Nanoparticles and in Situ Monitoring of Oriented Attachment. *J. Am. Chem. Soc.* **2011**, *133*, 14484−14487.
(28) Koh, W.; Yoon, Y.; Murray, C. B. Investigating the Phosphine Chemistry of Se Precursors for the Synthesis of PbSe Nanorods. *Chem. Mater.* **2011**, *23*, 1825−1829.
(29) Zherebetskyy, D.; Scheele, M.; Zhang, Y.; Bronstein, N.; Thompson, C.; Britt, D.; Salmeron, M.; Alivisatos, P.; Wang, L.-W. Hydroxylation of the surface of PbS nanocrystals passivated with oleic acid. *Science* **2014**, *344*, 1380−1384.
(30) Huang, X.; Zhu, J.; Ge, B.; Gerdes, F.; Klinke, C.; Wang, Z. In Situ Constructing the Kinetic Roadmap of Octahedral Nanocrystal Assembly Toward Controlled Superlattice Fabrication. *J. Am. Chem. Soc.* **2021**, *143*, 4234−4243.
(31) Rubin-Brusilovski, A.; Maikov, G.; Kolan, D.; Vaxenburg, R.; Tilchin, J.; Kauffmann, Y.; Sashchiuk, A.; Lifshitz, E. Influence of Alloying on the Optical Properties of IV−VI Nanorods. *J. Phys. Chem. C* **2012**, *116*, 18983−18989.
(32) Bartnik, A. C.; Efros, A. L.; Koh, W. K.; Murray, C. B.; Wise, F. W. Electronic states and optical properties of PbSe nanorods and nanowires. *Phys. Rev. B* **2010**, *82*, No. 195313.
(33) Dalven, R. A review of the semiconductor properties of PbTe, PbSe, PbS and PbO. *Infrared Phys.* **1969**, *9*, 141−184.
(34) Wehrenberg, B. L.; Wang, C.; Guyot-Sionnest, P. Interband and Intraband Optical Studies of PbSe Colloidal Quantum Dots. *J. Phys. Chem. B* **2002**, *106*, 10634−10640.
(35) de Mello, J. C.; Wittmann, H. F.; Friend, R. H. An improved experimental determination of external photoluminescence quantum efficiency. *Adv. Mater.* **1997**, *9*, 230−232.
(36) Sun, L.; Fang, J.; Reed, J. C.; Estevez, L.; Bartnik, A. C.; Hyun, B.-R.; Wise, F. W.; Malliaras, G. G.; Giannelis, E. P. Lead-Salt Quantum-Dot Ionic Liquids. *Small* **2010**, *6*, 638−641.

https://doi.org/10.1021/acsanm.1c02123
ACS Appl. Nano Mater. 2021, 4, 10708−10712